JOURNAL OF AIRCRAFT
Vol. 36, No. 2, March–April 1999

Modal Characteristics of a Flexible Smart Plate Filled with Electrorheological Fluids

Seung-Bok Choi*
Inha University, Incheon 402-751, Republic of Korea
Yong-Kun Park†
Myongji Junior College, Seoul 120-728, Republic of Korea
and
Sang-Bong Jung‡
Inha University, Incheon 402-751, Republic of Korea

This paper presents modal characteristics of a flexible smart plate filled with an electrorheological fluid. First, an oscillatory test is undertaken to extract the electric field-dependent complex shear modulus of the employed starch/silicone oil-based electrorheological fluid. A dynamic model of the smart plate associated with the measured modulus is then developed by adopting a finite element approach to predict field-dependent modal characteristics. Following the construction of a four-partitioned smart plate, an extensive modal test is empirically conducted to identify natural frequencies and mode shapes with respect to both the intensity and the area of the applied field to the fluid domains. Consequently, the measured natural frequencies and mode shapes are compared with the predicted ones to validate the proposed dynamic model. In addition, the control effectiveness for different field-energizing areas under the forced vibration is evaluated in the time domain.

Nomenclature

a = length of one finite element in x direction
b = length of one finite element in y direction
E_1 = Young's modulus of the aluminum
E_3 = Young's modulus of the composite laminate
G_2^* = complex shear modulus of the electrorheological fluid
h_1 = thickness of the aluminum
h_2 = thickness of the electrorheological fluid
h_3 = thickness of the composite laminate
T = kinetic energy of the smart plate
T_e = kinetic energy for one finite element
U = strain energy of the smart plate
U_b = bending strain energy of the aluminum and the composite laminate
U_e = axial strain energy of the aluminum and the composite laminate
U_s = shear strain energy of the electrorheological fluid
u_1 = in-plane displacement of the middle plane in the aluminum in x direction
u_3 = in-plane displacement of the middle plane in the composite laminate in x direction
$\tilde{V}$ = applied electric field to the electrorheological fluid domain
V_e = strain energy for one finite element
v_1 = in-plane displacement of the middle plane in the aluminum in y direction
v_3 = in-plane displacement of the middle plane in the composite laminate in y direction
w = transverse displacement
β_2 = shear loss factor of the electrorheological fluid
ν = Poisson's ratio of the aluminum and the composite laminate
ρ_1 = density of the aluminum
ρ_2 = density of the electrorheological fluid
ρ_3 = density of the composite laminate
ω = excitation frequency

Introduction

IN the area of aeronautics and astronautics, flexible structures have been extensively employed to satisfy various requirements for large scale, light weight, and high speed. However, these flexible structures are readily susceptible to the internal/external disturbances. Thus, vibration control schemes should be exerted by either an active or passive manner for higher accuracy, performance, and stability. As a typical passive methodology to deal with vibration suppression of flexible distributed-parameter structures, sandwich structures[1] with viscoelastic core materials and composite structures[2] with stacking process of laminae have been widely utilized. As a new methodology for active vibration control, smart structures[3] with their inherent adaptive capabilities to variable environments have made great progress in vibration control of flexible structural systems. Typically incorporated with aluminum, steel, and composite materials, smart structures have exploited piezoelectric sensing and actuating technologies, shape memory alloy actuators, electrorheological (ER) fluid actuators, and optical fiber sensing technology. As one of the principal ingredients, actuators are employed to dramatically tune the global or local mechanical properties and shapes of structural systems. Especially when it comes to the field of aerospace, embedded or surface-bonded actuators on an airplane wing or helicopter blade will induce alteration of twist/camber of airfoil, which in turn causes variation of lift distribution, and thus can help to control static and dynamic aeroelastic problems under stringent environments.[4,5]

In this paper, an ER fluid-embedded smart structure is proposed. The ER fluid itself exhibits a dramatic and reversible phase change in the presence of electric fields.[6] As well known,

Received May 28, 1998; revision received Sept. 14, 1998; accepted for publication Sept. 30, 1998.

*Associate Professor, Smart Structures and Systems Laboratory, Department of Mechanical Engineering.
†Assistant Professor, Department of Mechanical Design.
‡Graduate Student, Smart Structures and Systems Laboratory, Department of Mechanical Engineering.

embedded in voids of distributed-parameter structures, the ER fluid enables stiffness and damping properties of the structures to be instantly tuned by applying electric fields to the ER fluid domain. Because of the specific characteristics, numerous works have been accomplished in view of vibration control of distributed-parameter structures. Choi et al.[7] carried out experimental investigations on field-dependent modal characteristics of ER fluid-based cantilevered beams. The field-dependent natural frequencies, loss factor, and complex elastic modulus were evaluated at different volume fractions and particle concentrations of ER fluids, along with the deflection suppression through avoidance of the structural resonance by tailoring electric fields to ER fluid domains. Wereley[8] investigated the stiffness and damping characteristics of an ER fluid-filled rotor beam to demonstrate the feasibility of using ER fluids in vibration control of a flexible rotor blade system. Choi et al.[9] experimentally implemented an active control scheme for an ER fluid-based beam via measured field-dependent transfer function. As evident from the aforementioned works, most activities have been phenomenologically performed for cantilevered beams. Researches on the dynamic model and vibration control of ER fluid-based plate structures are considerably rare. Moreover, of the researches published, none deals with the tuning of mode shapes in a two-dimensional plate filled with ER fluids.

Consequently, the main objective of this study is to develop a dynamic model for predicting modal characteristics, and to implement shape control of an ER fluid-based smart plate. Firstly, a chemically treated starch/silicone oil-based ER fluid to be contained in the smart plate is composed and a rotary oscillation test is undertaken to extract the field-dependent complex shear modulus of the ER fluid itself as a function of excitation frequencies and applied fields. A dynamic model associated with the measured modulus is then formulated and solved through a finite element method. Following the construction of a four-partitioned smart plate, field-dependent modal properties such as natural frequencies are evaluated with respect to both the intensity and the area of the applied fields. This study's aim is to show how the field-dependent properties of the ER fluid itself can be employed to obtain controllable modal behaviors of two-dimensional structures in a globally or locally continuous fashion.

Dynamic Modeling

Viscoelasticity of ER Fluids

The ER fluid focused in this study consists of conducting particles and dispersing-insulating media, along with additives. The specific phenomenological effect of the ER fluid is characterized by its fast and reversible rheological properties in the presence of the electric field. Since Winslow's discovery of the ER effect,[6] numerous works have been accomplished to explain the effect through various experiments, theories, and assumptions. Based on these investigations on the ER effect, the constitutive behaviors of the ER fluid are typically expressed as a function of the field-dependent yield shear stress against shear strain and shear rate. Depending on the magnitude of the shear strain, the constitutive behavior of the ER fluid in shear can be largely divided into preyield and postyield regions. When the ER fluid is contained in the structural system under continuous and periodic small deformations, it remains in a preyield state of viscoelasticity, which can be controlled within a certain range by the applied electric field.[10] To infer the dynamic properties of the ER fluid itself in the distributed-parameter structural systems under vibration, a dynamic test to subject the ER fluid to an oscillatory shear strain is required to determine viscoelastic properties with complex shear modulus. Of the complex shear modulus, the storage shear modulus expresses the force among conducting particles, which is related to the stiffness characteristics of the ER fluid-embedded

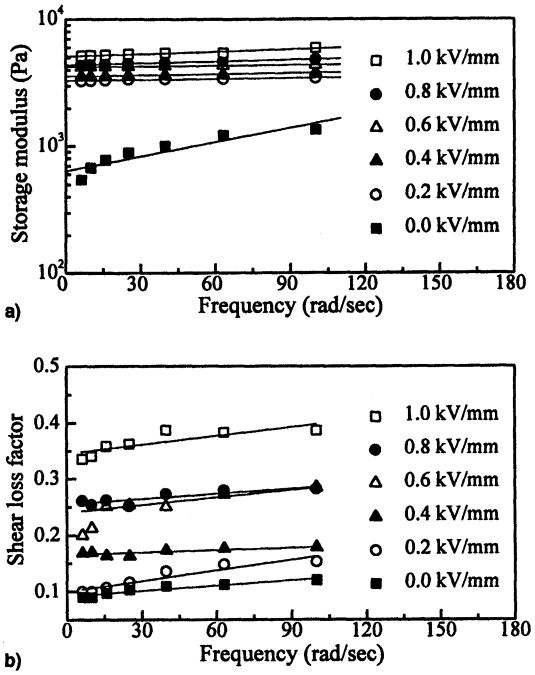

Fig. 1 Field-dependent complex shear modulus of the employed ER fluid: a) shear storage modulus and b) shear loss factor.

structure. The loss factor, namely, the ratio of energy lost and energy stored in a cycle of shear deformation, is associated with the damping characteristics of the ER fluid-based structural system.

In this study, a rotary oscillation test to extract the field-dependent rheological measurement was performed with the dynamic spectrometer. A chemically treated starch/silicone oil-based ER fluid is composed. The size of the starch particles ranges from 10 to 100 μm. The concentration of the particles is 55% by weight, and the viscosity of the silicone oil is 50 cS. The conductivity of the particles is $3.2-5.4 \times 10^{-10}\ \Omega^{-1}\ \text{cm}^{-1}$. The employed ER fluid is easily available, nontoxic, and eminent for field-dependent mechanical properties.[7] The ER fluid was placed in circular parallel plate fixtures with the diameter of 50 mm, where the gap between the fixtures is 1 mm. The experiment was undertaken via a constant sinusoidal strain method with a strain of 0.8% under a room temperature of 25°C. By sweeping oscillatory exciting frequencies of the fixtures, complex shear modulus was measured under the constant electric field from 0.0 kV/mm to 1.0 kV/mm at each 0.2 kV/mm increment. Figure 1 presents the measured complex shear modulus of the employed ER fluid. It is clearly shown that both the storage shear modulus and loss factor of the employed ER fluid vary with respect to the electric field ($\tilde{V}$) as well as the excitation frequency (ω). Similar to other ER fluids over the investigated frequency range, the storage shear modulus and shear loss factor increase with respect to the imposed field. This measured complex shear modulus is employed to formulate a dynamic model for predicting field-dependent modal characteristics of the ER fluid-filled plate structure.

Finite Element Formulation

A sandwich plate (Fig. 2), in which the ER fluid is contained between two elastic face layers of aluminum and composite laminate, is examined. The controllable modulus of the ER fluid can be used to tune structural behaviors of the sandwich plate in a continuous fashion, which is the primary motivation of this study. Like the previous approaches by Mead,[11] the following assumptions are also adopted to formulate a dynamic model of the smart plate.

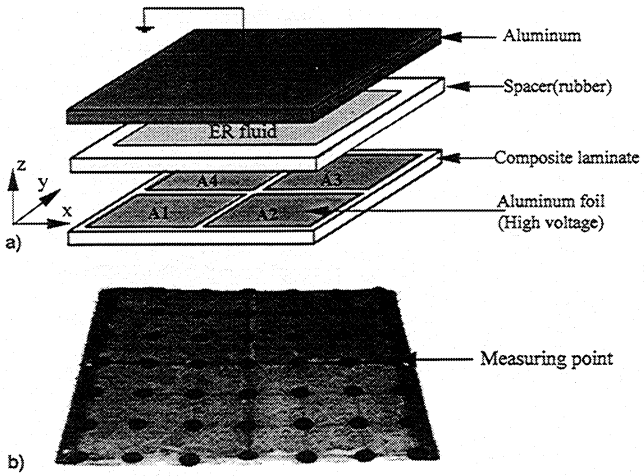

Fig. 2 Schematic diagram of the ER fluid-based smart plate: a) configuration and b) photograph.

1) The face layers suffer no transverse shear deformation.
2) The core material carries transverse shear, but no in-plane stresses.
3) The core material is linearly viscoelastic.
4) Because of perfect bonding, no slip occurs at the interfaces of the three layers.
5) Because of thin face layers and flexural vibration, in-plane inertia effects are ignored.

According to these fundamental assumptions, we can obtain strain and kinetic energies for the ER fluid-based plate. Strain energy of the smart plate is written as the sum of axial strain energy, bending strain energy of the face layers (the aluminum and composite laminate), and shear-strain energy of the core material (ER fluid)[12] as follows:

$$
\begin{aligned}
U &= U_e + U_b + U_s \\
&= \frac{1}{2}\frac{E_1 h_1}{(1-\nu^2)}\int\int\left[\left(\frac{\partial u_1}{\partial x}\right)^2 + 2\nu\frac{\partial u_1}{\partial x}\frac{\partial v_1}{\partial y}\right. \\
&\quad \left. + \left(\frac{\partial v_1}{\partial y}\right)^2 + \frac{(1-\nu)}{2}\left(\frac{\partial u_1}{\partial y} + \frac{\partial v_1}{\partial x}\right)^2\right] \mathrm{d}x\,\mathrm{d}y \\
&\quad + \frac{1}{2}\frac{E_3 h_3}{(1-\nu^2)}\int\int\left[\left(\frac{\partial u_3}{\partial x}\right)^2 + 2\nu\frac{\partial u_3}{\partial x}\frac{\partial v_3}{\partial y}\left(\frac{\partial v_3}{\partial y}\right)^2\right. \\
&\quad \left. + \frac{(1-\nu)}{2}\left(\frac{\partial u_3}{\partial y} + \frac{\partial v_3}{\partial x}\right)^2\right] \mathrm{d}x\,\mathrm{d}y \\
&\quad + \frac{1}{24(1-\nu^2)}(E_1 h_1^3 + E_3 h_3^3)\int\int\left[\left(\frac{\partial^2 w}{\partial x^2}\right)^2 + 2\nu\frac{\partial^2 w}{\partial x^2}\frac{\partial^2 w}{\partial y^2}\right. \\
&\quad \left. + \left(\frac{\partial^2 w}{\partial y^2}\right)^2 + 2(1-\nu)\left(\frac{\partial^2 w}{\partial x \partial y}\right)^2\right] \mathrm{d}x\,\mathrm{d}y \\
&\quad + \frac{1}{2}\frac{G_2^*(\tilde{V},\omega)}{h_2}\int\int\left[\left(u_1 - u_3 + \mathrm{d}_t\frac{\partial w}{\partial x}\right)^2\right. \\
&\quad \left. + \left(v_1 - v_3 + \mathrm{d}_t\frac{\partial w}{\partial y}\right)^2\right] \mathrm{d}x\,\mathrm{d}y \qquad (1)
\end{aligned}
$$

where $\mathrm{d}_t = (h_1 + h_3)/2 + h_2$. The kinetic energy of the plate is given by

$$
T = \frac{1}{2} m_t \int\int \left(\frac{\partial w}{\partial t}\right)^2 \mathrm{d}x\,\mathrm{d}y \qquad (2)
$$

Herein, $m_t = \rho_1 h_1 + \rho_3 h_3 + \rho_2 h_2$, which implies mass per unit area of the smart plate. Following the derivation of the strain and kinetic energies, the transverse displacement of the plate is to be described by shape functions and nodal displacements to formulate finite elements.

In this paper, a rectangular bending element with second-order twist derivatives is employed in which each corner node has four degrees of freedom. Define the nodal vector $\{q\}$ of the rectangular finite element as

$$
\{q\} = \left(w_i, \frac{\partial w}{\partial x_i}, \frac{\partial w}{\partial y_i}, \frac{\partial^2 w}{\partial x \partial y_i}\right)^T, \qquad i = 1, \ldots, 4 \qquad (3)
$$

The transverse displacement is assumed to be expressed as a 16-term polynomial displacement function, where the constants are determined by evaluating the 16-nodal values. The transverse displacement can be explicitly rewritten in terms of bicubic Hermitian shape functions $N(\xi, \eta)$ with nondimensional centroidal coordinates ξ and η[13]:

$$
w(\xi, \eta, t) = \sum_{i=1}^{4} N(\xi, \eta)_i q \qquad (4)
$$

Herein

$$
\begin{aligned}
\sum_{i=1}^{4} N(\xi,\eta)_i = \sum_{i=1}^{4}\Bigg[& G_i(\xi)G_i(\eta) + \frac{a}{2}H_i(\xi)G_i(\eta) \\
& + \frac{b}{2}G_i(\xi)H_i(\eta) + \frac{ab}{4}H_i(\xi)H_i(\eta)\Bigg] \qquad (5)
\end{aligned}
$$

In the preceding equation

$$
\begin{gathered}
G_i(\xi) = (-\xi_i\xi^3 + 3\xi_i\xi + 2)/4, \quad H_i(\xi) = (\xi^3 + \xi_i\xi^2 - \xi - \xi_i)/4 \\
\xi = 2(x/a) - 1, \quad \eta = 2(y/b) - 1 \\
G_i(\eta) = (-\eta_i\eta^3 + 3\eta_i\eta + 2)/4 \\
H_i(\eta) = (\eta^3 + \eta_i\eta^2 - \eta - \eta_i)/4
\end{gathered}
$$

On the other hand, because of strain compatibility on the interfaces among the three layers, the relationship between in-plane displacement and transverse displacement is given by

$$
\begin{aligned}
\frac{\mathrm{d}^2 u_1}{\mathrm{d}x^2} - \frac{G_2^*(\tilde{V},\omega)}{E_1E_3h_1h_2h_3}(E_1h_1 - E_3h_3)u_1 &= -\frac{G_2^*(\tilde{V},\omega)\mathrm{d}_t}{E_1h_1h_2}\frac{\partial w}{\partial x} \\
\frac{\mathrm{d}^2 v_1}{\mathrm{d}y^2} - \frac{G_2^*(\tilde{V},\omega)}{E_1E_3h_1h_2h_3}(E_1h_1 - E_3h_3)v_1 &= -\frac{G_2^*(\tilde{V},\omega)\mathrm{d}_t}{E_1h_1h_2}\frac{\partial w}{\partial y}
\end{aligned} \qquad (6)
$$

With the aid of Eqs. (4) and (6), and Eqs. (1) and (2), the strain and kinetic energies for one rectangular finite element structure can be rewritten, respectively, in terms of the nodal displacement $\{q\}$ as follows:

$$
V_e = \{q\}^T([k_1] + [k_2] + [k_3])\{q\}/2, \quad T_e = \{\dot{q}\}^T[m]\{\dot{q}\}/2 \qquad (7)
$$

where the stiffness matrices $[k_1]$, $[k_2]$, and $[k_3]$ from the bending, axial, and shear strain energies, respectively, and the mass matrix $[m]$ are symmetric with size of 16×16. It is well noted that the stiffness matrices $[k_2]$ and $[k_3]$, associated with the complex shear modulus of the ER fluid in Fig. 1, are a function of the applied electric fields as well as excitation frequencies. By introducing Lagrange's equation and incorporating a structural damping effect of the core material (the ER fluid) of β_2, the governing equation for one finite element can be expressed by

$$
[m]\{\ddot{q}\} + ([k_1] + [k_2] + [k_3] + i\beta_2([k_2] + [k_3]))\{q\} = \{0\} \qquad (8)
$$

The system equation for the total structure can be obained by assembling all governing equations for each element. In addition, because of the frequency dependence of the stiffness matrices $[k_2]$ and $[k_3]$, it is reasonable to consider the forced vibration in the frequency domain rather than in the time domain, which has a nonzero force vector on the right-hand side of Eq. (8) given as

$$[M]\{\ddot{Q}\} + ([K_1] + [K_2] + [K_3] + i\beta_2([K_2] + [K_3]))\{Q\} = \{f\} \tag{9}$$

Substituting an excitation force vector ($\{f\} = \{\bar{F}\}e^{i\omega t}$) and a structural response ($\{Q\} = \{\bar{Q}\}e^{i\omega t}$) into Eq. (9) and factoring-out time-dependent parts, a frequency response equation can be determined as

$$\{\bar{Q}\} = (-\omega^2[M] + [K_1] + [K_2] + [K_3] + i\beta_2([K_2] + [K_3]))^{-1}\{\bar{F}\} \tag{10}$$

Letting the jth components of $\{F\}$ be excitation terms, a frequency response H_{ij} at the ith position of the structure can be found by

$$H_{ij} = \bar{Q}_i/\bar{F}_j \tag{11}$$

Experimental Setup and Procedures

Figure 2a illustrates a schematic configuration of the proposed ER fluid-based smart plate, which consists of a rubber spacer, an ER fluid, and two elastic face layers of aluminum and glass/epoxy composite laminate. The upper aluminum layer provides rigidity as a host material and also serves as an electrode of common electric field, and the silicone rubber spacer acts as a seal to hold the integrity of the structure, as well as an electrical insulator. The rubber spacer is perfectly bonded to the face layers with a silicone room temperature vulcanite adhesive. On the other hand, the composite laminate layer is coated with very thin aluminum foils (0.018 mm) partitioned into four parts, which independently provide different positive electric fields to the ER fluid domain. The parts of the separated foils are numbered counterclockwise as *A*1, *A*2, *A*3, and *A*4. Into the void between the two face layers, the chemically treated starch/silicone oil-based ER fluid is inserted. The volume fraction of the ER fluid to the total structure is 75%. Table 1 presents dimensions and material properties of the proposed smart plate components. Herein, the concentration of the ER fluid implies the weight ratio of the particle (starch) to the ER fluid. The volume fraction of the ER fluid to the total specimen is controlled by adjusting the width and thickness of the rubber spacer between the aluminum and the composite laminate. In fact, the composition of the ER fluid and the volume fraction are very important parameters in determining field-dependent elastodynamic properties of ER fluid-based structures.

Figure 3 shows an overall view for the experimental apparatus employed to investigate field-dependent modal characteristics of the ER fluid-based plate. The smart plate is mounted to a fixture on clamped–clamped boundary conditions along two opposite sides. The rigid fixture is bolted on the shaker. Both the fixture and the shaker are insulated from the applied electric fields. A proximitor is located on the fixture to

Table 1 Dimensions and mechanical properties of the ER fluid-based plate

Specification	Aluminum	Composite laminate	ER fluid
Young's modulus, GPa	6.2	32	——
Poisson's ratio	0.3	0.3	——
Density, kg/m^3	2652	1850	1145
Thickness, mm	0.25	0.5	3.60
Width, mm	400	400	390
Length, mm	400	400	390
Base oil	——	——	Silicone oil
Particle	——	——	Starch
Volume fraction, %	——	——	75
Particle concentration, %	——	——	55

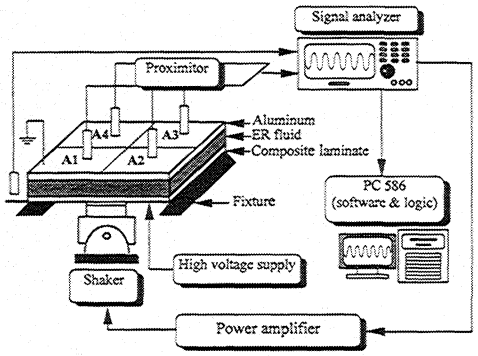

Fig. 3 Overall experimental setup.

Table 2 Field-dependent modal parameters at different field energizing areas

Field area	Input field, kV/mm	Experiment (Hz) mode (1, 1)	(1, 2)	(2, 1)	(2, 2)	Prediction (Hz) mode (1, 1)	(1, 2)	(2, 1)	(2, 2)
None	0.0	11.12	12.55	37.67	48.67	11.00	14.01	37.99	49.00
A1 only	0.6	11.39	14.48	42.58	56.33	11.06	15.98	40.68	54.86
	0.8	11.42	18.01	43.58	59.33	11.18	16.76	42.21	57.45
	1.0	11.54	19.16	43.94	65.41	11.24	17.85	44.45	59.60
A1, A2	0.6	11.50	13.87	43.73	60.22	11.36	16.68	41.55	55.21
	0.8	11.60	17.96	44.48	60.55	11.55	17.22	42.98	57.68
	1.0	11.63	19.23	45.74	61.43	11.61	18.98	44.42	60.11
A1, A3	0.6	11.51	13.39	44.74	57.12	11.29	15.98	41.24	55.65
	0.8	11.58	14.13	46.81	62.59	11.41	17.42	43.88	58.88
	1.0	11.65	14.20	47.29	65.70	11.55	18.76	44.55	60.02
A1, A4	0.6	11.59	13.44	47.37	59.19	11.21	16.65	41.12	55.11
	0.8	11.62	14.50	47.46	61.83	11.38	17.88	43.30	58.02
	1.0	11.68	14.96	48.42	69.95	11.54	18.52	45.00	60.21
A1, A3, A4	0.6	11.67	14.01	46.02	61.09	11.32	16.86	41.65	55.02
	0.8	11.70	17.33	46.08	62.05	11.45	18.02	43.10	57.68
	1.0	11.71	21.41	47.14	67.20	11.62	19.09	44.90	60.11
Area all	0.6	11.70	13.47	40.75	53.82	11.21	17.28	41.87	56.20
	0.8	11.73	13.69	42.53	60.56	11.68	18.42	43.02	58.24
	1.0	11.82	19.07	44.61	75.71	11.75	19.66	44.93	60.45

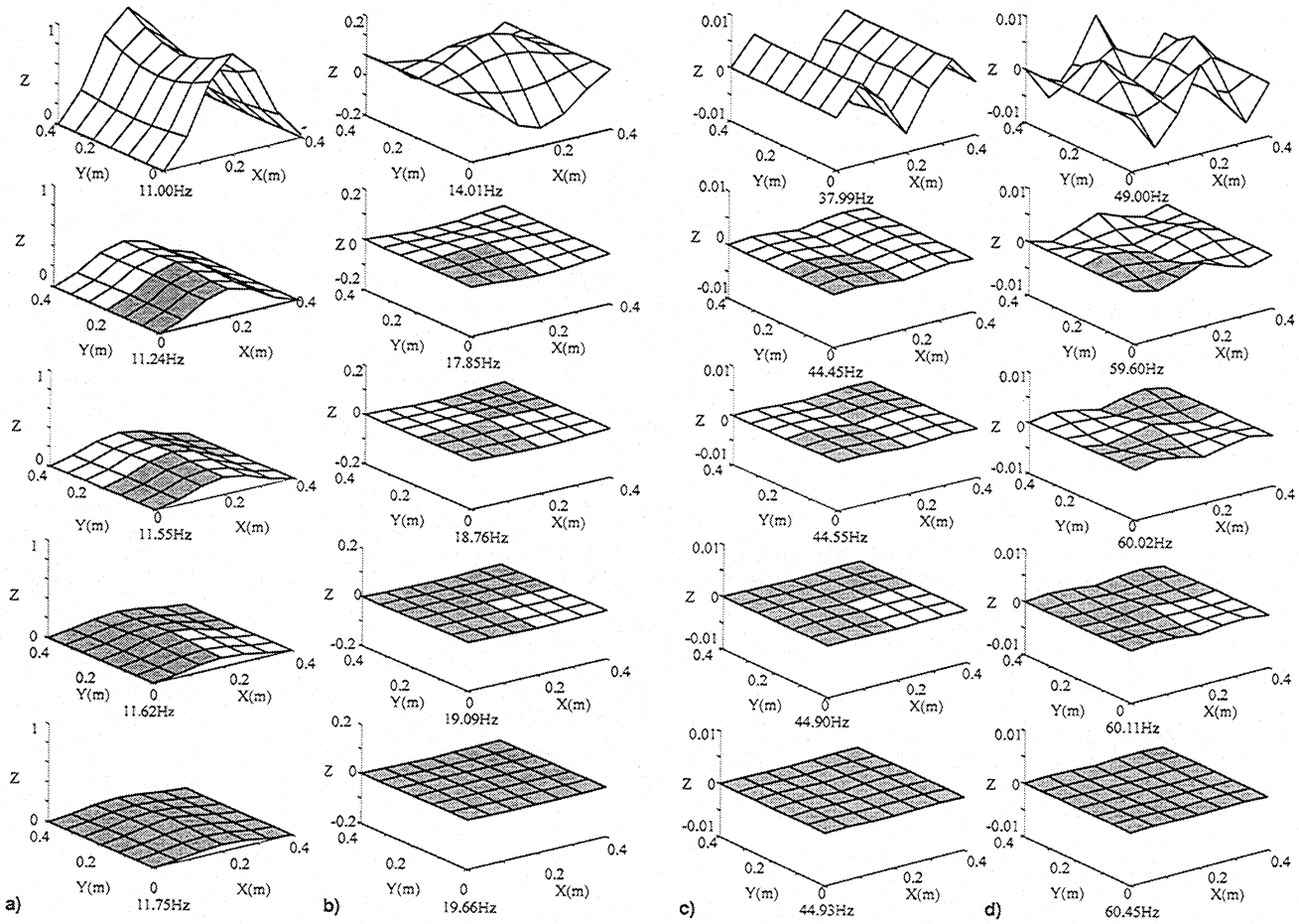

Fig. 4 Predicted mode shapes at different field energizing areas. Mode a) (1, 1); b) (1, 2); c) (2, 1); and d) (2, 2).

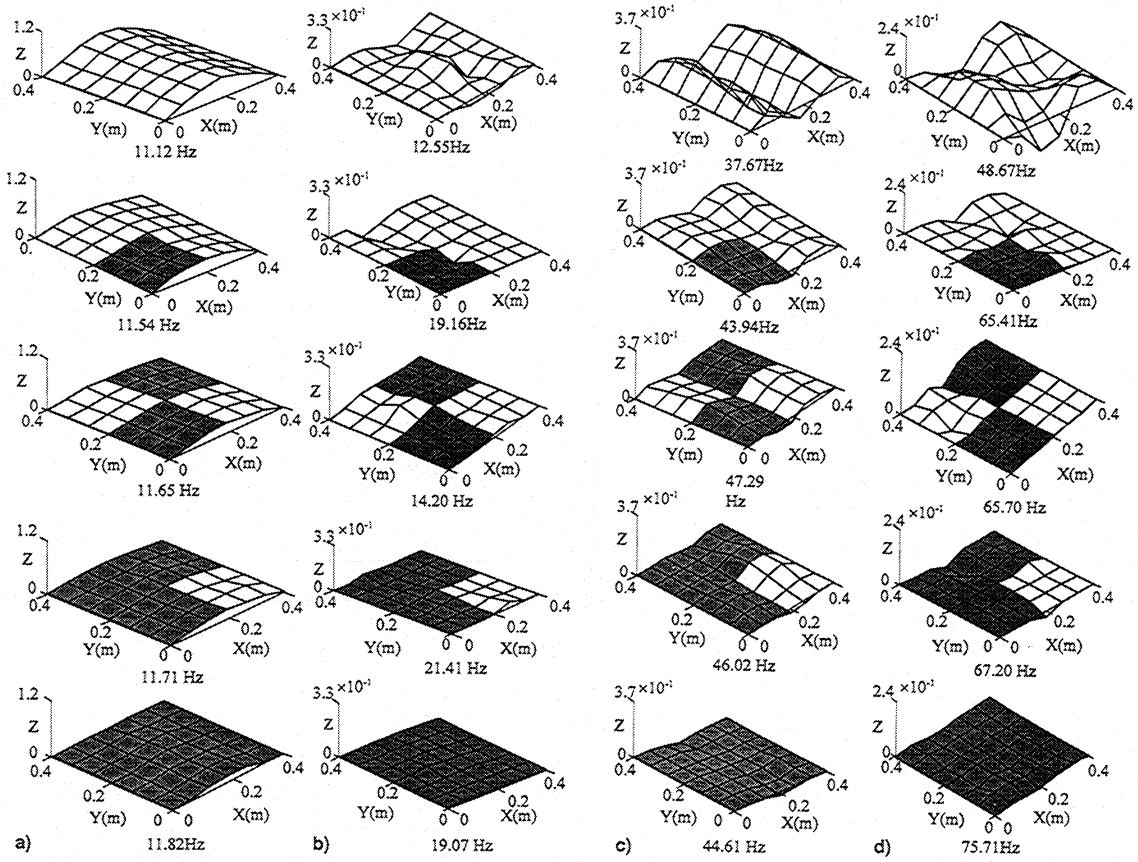

Fig. 5 Measured mode shapes at different field energizing areas. Mode a) (1, 1); b) (1, 2); c) (2, 1); and d) (2, 2).

measure the input signal and another probe is set over the plate to pick up vibration responses. The shaker is excited with random signals from the dynamic signal analyzer through the power amplifier. Both the input and output signals from the two proximitors are used to obtain frequency responses (transfer functions) at an interested position over the focused frequency span of 0–100 Hz, which contains the first four modes of the smart plate. With the aid of system software installed on a microcomputer, the measured transfer functions at each node point (total 49 node points, refer to Fig. 2b) are used to infer mode shapes and natural frequencies. To determine natural modes in heavy modal coupling, a coherence method is employed. High-voltage supplies independently furnish the smart plate with high electric fields in a continuous/discrete fashion. Considering both the effect of deflection suppressions and the measuring range of the proximitors, the random excitation magnitude is appropriately limited to an rms of 2.30 m/s^2. Field-dependent transfer functions are measured by increasing electric fields from 0.0 to 1.0 kV/mm at each 0.2-kV/mm increment. On the basis of the fact that the employed ER fluid easily changes into a solid phase at a low electric field because of the high particle concentration of 55%, 1.0 kV/mm is appropriately chosen as a maximum electric field.

Results and Discussions

Consider a square ER fluid-based plate, of which two opposite sides are clamped–clamped and the others are free. The size of the plate is 400 mm by 400 mm with a total thickness of 4.35 mm. Thirty-six rectangular elements of a 6 × 6 array with 49 nodes are employed to form a mesh (refer to Fig. 2b). Each node with four degrees of freedom is numbered consecutively along the x axis, which leads to 196 degrees of freedom. For the analytical case, the position of harmonic force excitation and structure response is the center of the plate. With the aid of transfer functions obtained from the experiment and from the dynamic finite element model, natural frequencies and mode shapes can be inferred. In this study, the first four natural modes dominant in flexural vibrations of the proposed smart plate are considered. Table 2 represents the first four predicted and measured natural frequencies with respect to both the intensity and the area of applied electric fields. It is well noted that various modal frequencies can be accomplished as a function of the energizing area as well as the intensity of the imposed electric field. As the field intensity and the applied area become larger, the modal frequencies increase. For instance, note from the measured data that the fouth natural frequency of 48.67 Hz without electric field increases to 75.71 Hz by applying the electric field of 1.0 kV/mm to all of the areas. There is a good agreement between measured and predicted results. The minor discrepancy comes mainly from neglecting the fixture, the silicone rubbber spacer, and the thin aluminum foils in formulating the dynamic model.

Similar to the case of the modal frequencies, we obtain various mode shapes as a function of the energizing area as well as the intensity of the imposed field. In this paper, under the employed maximum field of 1.0 kV/mm, mode shapes tuned by different field-energizing areas are exhibited. Figures 4 and 5 denote predicted and measured mode shapes by globally and locally applying the field of 1.0 kV/mm. The shaded zones illustrate the areas subjected to the electric field. Amplitude of mode shape is normalized with respect to amplitude of mode (1, 1). As expected, the suppression of mode shapes becomes larger with increment of the energizing areas. Under the same electric field of 1.0 kV/mm, various mode shapes are obtained by only changing the energizing areas. The difference between the predicted and measured mode shapes arises from the fact that single-point excitation with sine sweeping is employed in the dynamic model, whereas two fixed-edges excitation with random signal is adopted in the experiment. Because complex shear modulus of the ER fluid can be measured through a sine sweeping method, the sine sweeping excitation method is adopted in obtaining the predicted mode shapes. As evident from the results, a desired mode shape can be accomplished by combination of the intensity and the energizing area of the applied electric field. This is the most eminent modal characteristic of the proposed smart plate. Figure 6 presents the measured responses at the center of node 25 in the time domain under mode (1, 1) excitation of 11.12 Hz. Under the field of 1.0 kV/mm, various responses for the suppression of the point deflection are obtained with respect to the energizing areas. Because of the increment of stiffness and damping properties, vibration alleviation becomes higher as the energizing areas increase.

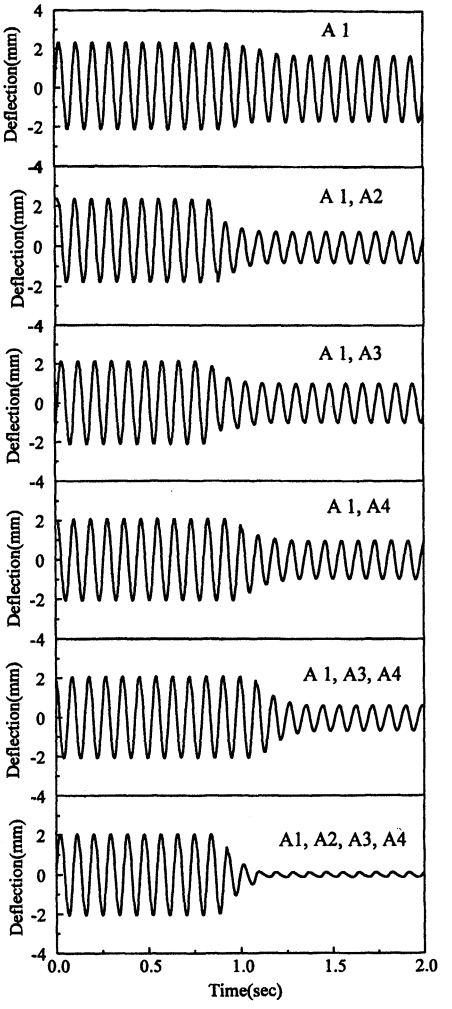

Fig. 6 Measured deflection suppression under the forced vibration at different field energizing areas.

The results presented in this study indicate that by applying electric fields with an appropriate control scheme, mode shapes and vibrational behaviors of flexible structural systems can be arbitrarily tuned. These capabilities will be very important in applications of various aerospace structures such as aircraft wing and rotor blades subjected to either global or local disturbances and parameter variations.

Conclusions

A dynamic model of an ER fluid-based smart plate was proposed to predict modal characteristics such as natural frequency and mode shape. To demonstrate the effectiveness of the smart plate and dynamic model, globally and locally controlled mode shapes and natural frequencies were investigated through both simulation and experiment. The predicted and experimental results provide the feasibility of controlling the vibration characteristics of flexible structural systems via an

ER fluid actuator. As a second phase of this study, an appropriate control scheme for controlling the mode shapes is to be developed in a closed-loop feedback manner.

References

[1]Douglas, B. E., and Yang, J. C. S., "Transverse Compressional Damping in the Vibratory Response of Viscoelastic-Elastic Beams," *AIAA Journal*, Vol. 16, No. 9, 1978, pp. 925–930.

[2]Vinson, J. R., and Chou, T. W., *Composite Materials and Their Use in Structures*, Wiley, New York, 1975.

[3]Gandhi, M. V., and Thompson, B. S., *Smart Materials and Structures*, Chapman & Hall, London, 1992, pp. 70–136.

[4]Lazaraus, K. B., Saarmaa, E., and Agnes, G. S., "Active Smart Material System for Buffet Load Alleviation," *Proceedings of the SPIE's 95 Symposium on Smart and Structures and Materials*, Vol. 2447, International Society for Optical Engineering, San Diego, CA, 1995, pp. 179–192.

[5]Jardine, A. P., Flanagan, J., Martin, C. A., and Carpenter, Bernie, F., "Smart Wing Shape Memory Alloy Actuator Design and Performance," *Proceedings of the SPIE's 97 Symposium on Smart and Structures and Materials*, Vol. 3044, International Society for Optical Engineering, San Diego, CA, 1997, pp. 48–55.

[6]Winslow, W. M., "Induced Fibration Suspensions," *Journal of Applied Physics*, Vol. 20, No. 12, 1947, pp. 1137–1140.

[7]Choi, S. B., Park, Y. K., and Suh, M. S., "Elastodynamic Characteristics of Hollow Cantilever Beams Containing an Electro-Rheological Fluid: Experimental Results," *AIAA Journal*, Vol. 32, No. 2, 1994, pp. 438–440.

[8]Wereley, N. M., "Active Damping of Flexible Rotor Blades Using Electrorheological—Fluid-Based Actuators," *Proceedings of the SPIE's 94 Symposium on Smart Structures and Materials*, Vol. 2190, International Society for Optical Engineering, Orlando, FL, 1994, pp. 13–18.

[9]Choi, S. B., Park, Y. K., and Cheong, C. C., "Active Vibration Control of Intelligent Composite Laminate Structures Incorporating an Electro-Rheological Fluid," *Journal of Intelligent Material Systems and Structures*, Vol. 7, No. 4, 1996, pp. 411–419.

[10]Gamota, D. R., and Filisko, F. E., "Dynamic Mechanical Studies of Electro-Rheological Materials: Moderate Frequency," *Journal of Rheology*, Vol. 35, No. 3, 1991, pp. 399–425.

[11]Mead, D. J., "The Damping Properties of Elastically Supported Sandwich Plates," *Journal of Sound and Vibration*, Vol. 24, No. 2, 1972, pp. 275–295.

[12]He, J. F., and Ma, B. A., "Analysis of Flexible Vibration of Viscoelastically Damped Sandwich Plates," *Journal of Sound and Vibration*, Vol. 120, No. 1, 1988, pp. 37–47.

[13]Yang, T. Y., *Finite Element Structural Analysis*, Prentice–Hall, Englewood Cliffs, NJ, 1986, pp. 399–480.